

# Two-scale numerical solution of the electromagnetic two-fluid plasma-Maxwell equations: Shock and soliton simulation

S. Baboolal<sup>a,\*</sup>, R. Bharuthram<sup>b</sup>

<sup>a</sup> School of Computer Science, University of KwaZulu-Natal, Westville Campus, Private Bag X54001, Durban 4000, South Africa

<sup>b</sup> Faculty of Science, University of the Witwatersrand, Private Bag 3, Wits 2050, Johannesburg, South Africa

Available online 16 January 2007

## Abstract

Here, we indicate how to integrate the set of conservation equations for mass, momentum and energy for a two-fluid plasma coupled to Maxwell's equations for the electromagnetic field, written in a composite conservative form, by means of a recently modified non-staggered version of the staggered second order central difference scheme of Nessyahu and Tadmor [H. Nessyahu, E. Tadmor, Non-oscillatory central differencing for hyperbolic conservation laws, *J. Comput. Phys.* 87 (1990) 408–463]. Allowing for wave propagation in one dimension, we illustrate the formation and evolution of magnetosonic shocks and solitons using two sets of time and space normalizations.

© 2007 IMACS. Published by Elsevier B.V. All rights reserved.

MSC: 35L65; 65M06; 74J35; 74J40; 76W05; 76X05

Keywords: Shocks; Solitons; Plasma-Maxwell equations; High-resolution scheme

## 1. Introduction

Solitons and shocks are observed in various fluids including plasmas, which can be treated as multi-species ionized fluids subject to the laws of electrodynamics. Magnetosonic waves arise when propagation is observed in a direction, say  $x$ , and are driven by a transverse magnetic field in a direction, say  $y$ , coupled with a transverse electric field component in the other direction,  $z$ . The plasma then undergoes rarefactions and compressions in the  $x$  direction due to the so-called “ $E \times B$  drift” [3]. Theory, experiments and simulations [3,6,7,2] show that solitons and shocks occur both in the laboratory and space.

In the past [6], a Lax-Wendroff scheme was employed in the numerical simulation of magnetosonic solitons, and recently [7], an approximate Riemann solver was used to numerically integrate a two-fluid plasma system to model magnetosonic shocks. A Riemann-solver-free scheme was employed on a single-fluid system to study magneto-hydrodynamic (MHD) shocks [2]. Here, we employ a similar but non-staggered version [4] of the method of Nessyahu and Tadmor [5] on a two-fluid plasma system to model both shocks and solitons. However, another thrust of these studies is to examine the impact of the differing time scales induced by the widely disparate electron and ion masses.

\* Corresponding author.

E-mail addresses: [baboolals@ukzn.ac.za](mailto:baboolals@ukzn.ac.za) (S. Baboolal), [bharuthramr@science.wits.ac.za](mailto:bharuthramr@science.wits.ac.za) (R. Bharuthram).

## 2. The numerical integration scheme

For numerical study we write the system of equations in the conservative form,

$$\frac{\partial U(x, t)}{\partial t} + \frac{\partial F(U)}{\partial x} = G(U) \quad (1)$$

where  $U(x, t)$  is the unknown ( $m$ -dimensional) vector,  $F(U)$  the flux vector and  $G(U)$  is a source vector, with  $x$  the space and  $t$  the time coordinate. On this form, we can use the recently modified scheme [4], namely a non-staggered source-term-inclusive variation form of [5]:

$$\begin{aligned} \bar{U}_j^{n+1} &= \frac{1}{4}[\bar{U}_{j+1}^n + 2\bar{U}_j^n + \bar{U}_{j-1}^n] - \frac{1}{16}[U_{xj+1}^n - U_{xj-1}^n] \\ &\quad - \frac{1}{8}[U_{xj+(1/2)}^{n+1} - U_{xj-(1/2)}^{n+1}] + \frac{\Delta t}{8}[G_{j+1}^n + 2G_j^n + G_{j-1}^n] + \frac{\Delta t}{8}[G_{j+1}^{n+1} + 2G_j^{n+1} + G_{j-1}^{n+1}] \\ &\quad - \frac{\Delta t}{4\Delta x}[(F_{j+1}^n - F_{j-1}^n) + (F_{j+1}^{n+1} - F_{j-1}^{n+1})] \end{aligned} \quad (2)$$

This scheme advances the cell average vectors  $\bar{U}_j^n$  (see ref. [5]), where  $j$  is the spatial discretization index with grid spacing  $\Delta x$ ,  $n$  the time level index, with time spacing  $\Delta t$ , and it is used in conjunction with the derivative array approximations ( $U_x$ ) (see refs. [4,5] for details). Also required is a predictor such as [5],

$$U^{n+1} = U^n + \Delta t \left[ G(U^n) - \frac{1}{\Delta x} F_x^n \right]. \quad (3)$$

The predicted flux vector values are obtained by employing  $F^{n+1} = F(U^{n+1})$  and the flux derivative terms  $F_x^n$  are approximated just as we do for  $U_x$  [4,5].

## 3. The electromagnetic plasma fluid equations

The model equations employed are Maxwell equations for the electromagnetic fields  $E = [E_x, E_y, E_z]^T$  and  $B = [B_x, B_y, B_z]^T$  coupled to the ideal-gas, collisionless-fluid equations for the electrons ( $s = e$ ) and ions ( $s = i$ ) in terms of  $n_s, V_s = [v_{sx}, v_{sy}, v_{sz}]^T, p_s, \gamma_s, m_s$  which are the respective component number densities, flow velocities, partial pressures, adiabatic indices and particle masses with particle charges taken as  $-e$  (electrons) and  $+e$  (ions). Further, we take  $\gamma_e = \gamma_i = \gamma$  as the adiabatic indices,  $p_e = n_e k_B T_e$  and  $p_i = n_i k_B T_i$  as the respective electron and ion partial pressures for ideal fluids, with their temperatures given as  $T_e = m_e V_{Te}^2 / k_B$  and  $T_i = m_i V_{Ti}^2 / k_B$ , where  $V_{Te}$  and  $V_{Ti}$  denote the root-mean-square thermal speeds for each species. These equations are reduced to components, but allowing for wave disturbances in the  $x$ -direction with  $\partial/\partial y \equiv 0$  and  $\partial/\partial z \equiv 0$ . Thereafter, we employ normalizations corresponding to time and spatial scales appropriate for the observation of magneto-sonic wave structures, to render them dimensionless.

In the first of these schemes (“ $e$ -scale”), we consider normalizations on a fast time scale corresponding to the electron plasma wave oscillation period. Here, the electron and ion densities are given in terms of  $n_0$  their common equilibrium density, lengths ( $x$ ) are in units of the electron Debye length  $\lambda_{de} = \sqrt{\epsilon_0 k_B T_{e0} / n_0 e^2} = \sqrt{\epsilon_0 m_e V_{Te0}^2 / n_0 e^2}$ , where  $\epsilon_0$  is the electric permittivity in free space and  $T_{e0}$  is the equilibrium electron temperature, temperatures are given in terms of  $T_{e0}$ , particle charges in terms of  $e > 0$  the electronic charge, time ( $t$ ) is in units of the inverse of the electron plasma frequency  $\omega_{pe} = \sqrt{n_0 e^2 / \epsilon_0 m_e}$ , velocities are in units of the electron thermal speed at equilibrium  $V_{Te0} = \sqrt{k_B T_{e0} / m_e}$ , and we take  $\gamma = 5/3$  for adiabatic fluids. Components of the electric field are in units of  $E_0 = \sqrt{m_e n_0 V_{Te0}^2 / \epsilon_0}$ , those of the magnetic field are in units of  $B_0 = E_0 / c$ , where  $c$  is the unnormalized speed of light, and we take  $r_s = m_e / m_s$  as the mass ratios ( $= 1$  for electrons,  $m_e / m_i$  for ions) and  $\sigma_s$  as the normalized charge ( $= -1$  for electrons,  $+1$  for ions). With normalized energy-per-mass terms,  $w_s = n_s |V_s|^2 + 3n_s V_{Ts}^2$ , the final 16-equation set then takes the form, similar to those in refs. [6,7]:

$$\frac{\partial}{\partial t}[n_s] + \frac{\partial}{\partial x}[n_s v_{sx}] = 0 \quad (4)$$

$$\frac{\partial}{\partial t}[n_s v_{sx}] + \frac{\partial}{\partial x} \left[ \frac{(n_s v_{sx})^2}{n_s} + n_s V_{Ts}^2 \right] = \sigma_s r_s \left[ E_x n_s + \frac{n_s v_{sy} B_z}{c} - \frac{n_s v_{sz} B_y}{c} \right] \quad (5)$$

$$\frac{\partial}{\partial t}[n_s v_{sy}] + \frac{\partial}{\partial x} \left[ n_s v_{sy} \frac{n_s v_{ex}}{n_s} \right] = \sigma_s r_s \left[ E_y n_s + \frac{n_s v_{sz} B_x}{c} - \frac{n_s v_{sx} B_z}{c} \right] \quad (6)$$

$$\frac{\partial}{\partial t}[n_s v_{sz}] + \frac{\partial}{\partial x} \left[ n_s v_{sz} \frac{n_s v_{sx}}{n_s} \right] = \sigma_s r_s \left[ E_z n_s + \frac{n_s v_{sx} B_y}{c} - \frac{n_s v_{sy} B_x}{c} \right] \quad (7)$$

$$\frac{\partial}{\partial t}[w_s] + \frac{\partial}{\partial x} \left[ w_s \frac{n_s v_{sx}}{n_s} + 2V_{Ts}^2 (n_s v_{sx}) \right] = 2\sigma_s r_s n_s [v_{sx} E_x + v_{sy} E_y + v_{sz} E_z] \quad (8)$$

$$\frac{\partial}{\partial t}[E_x] = n_e v_{ex} - n_i v_{ix}; \quad \frac{\partial}{\partial t}[E_y] + \frac{\partial}{\partial x}[c B_z] = n_e v_{ey} - n_i v_{iy} \quad (9)$$

$$\frac{\partial}{\partial t}[E_z] + \frac{\partial}{\partial x}[-c B_y] = n_e v_{ez} - n_i v_{iz}; \quad \frac{\partial}{\partial t}[B_x] + \frac{\partial}{\partial x}[0] = 0 \quad (10)$$

$$\frac{\partial}{\partial t}[B_y] + \frac{\partial}{\partial x}[-c E_z] = 0; \quad \frac{\partial}{\partial t}[B_z] + \frac{\partial}{\partial x}[c E_y] = 0. \quad (11)$$

We write this set in the conservation form (1) with the notation,

$$U = [u_1, u_2, u_3, u_4, u_5, u_6, u_7, u_8, u_9, u_{10}, u_{11}, u_{12}, u_{13}, u_{14}, u_{15}, u_{16}]^T \\ \equiv [n_e, n_i, n_e v_{ex}, n_e v_{ey}, n_e v_{ez}, n_i v_{ix}, n_i v_{iy}, n_i v_{iz}, w_e, w_i, E_x, E_y, E_z, B_x, B_y, B_z]^T \quad (12)$$

and with consequential forms for  $F(U)$  and  $G(U)$ .

In the second normalization scheme (“ $i$ -scale”), with time in terms of the inverse of the slower ion plasma frequency  $\omega_{pi} = \sqrt{n_0 e^2 / \epsilon_0 m_i}$ , length as before and velocities in terms of the ion sound speed at equilibrium  $C_{s_0} = \sqrt{m_e V_{Te_0}^2 / m_i}$ , the only changes to the basic equations occur in the mass ratio factors  $r_s$  on the right of the above equations where now  $r_s = r_i = 1$  for ions and  $r_s = r_e = m_i / m_e$  for the electrons.

At this juncture, we note that the system of equations above, culminating in (1) is not locally hyperbolic. In fact for its flux Jacobian it can be shown that the eigenvalues are not all real and distinct. This may be inferred from the Maxwell equations subset (9)–(11). Nevertheless, although the numerical scheme used here [4] is based on ref. [5] whose theoretical foundation assumes the system dealt with is hyperbolic, hyperbolicity is a sufficiency condition in the latter stability and convergence theory. Thus, we can still expect the schemes to function under weaker conditions. In fact our results bear testimony to this. Moreover, linear stability analysis of the scheme [5] indicates that it should remain stable under the CFL condition  $\Lambda_m \Delta t / \Delta x \leq 0.5$ , where  $\Lambda_m$  is the spectral radius of the flux Jacobian, which is stronger than that for the Lax-Wendroff scheme used in electrostatic simulations [1]. Now, for the numerical integration, we employ a system of size  $L_x = 128$  ‘volumes’, each of size a Debye length  $\lambda_{de}$ , with the number of grid points per volume of  $N_{px} = 20$ , giving  $\Delta x = 0.05$ , an artificial ion-to-electron mass ratio of 10:1, an ion-to-electron temperature ratio of 1:10 together with  $\Delta t = 0.005$ . Further, to compute with this scheme we have to employ an implicit procedure similar to [4,1]. The interesting variation here from the work of Shumlak and Loverich [7] is that the complete system of equations is solved as if we are dealing with a hyperbolic system such as (1).

#### 4. Magnetosonic shock and soliton computations

For shocks, we employ the initial conditions with  $c = 10$ , corresponding to a ‘very hot’ plasma, together with zero initial flow velocities and free boundary conditions, corresponding to a Riemann (shock-tube or two-state plasma)

problem with a discontinuity at the system centre  $x_c$ :

$$\begin{cases} n_e = 4, n_i = 4, V_e = 0, V_i = 0, w_e = 3n_e V_{Te0}^2, w_i = 3n_i V_{Ti0}^2, \\ E_x = 0, E_y = 0, E_z = 0, B_x = 0, B_y = 1, B_z = 0; & x \leq x_c. \\ n_e = 1, n_i = 1, V_e = 0, V_i = 0, w_e = 3n_e V_{Te0}^2, w_i = 3n_i V_{Ti0}^2, \\ E_x = 0, E_y = 0, E_z = 0, B_x = 0, B_y = 1, B_z = 0; & x > x_c. \end{cases}$$

For soliton computations, we change only the initial density profile to a Gaussian (centred “hump”) for each component,

$$n_s(x, 0) = 1.0 + 4.0 \exp \left[ -\frac{1}{2}(x - x_c)^2 \right]; \quad 0 \leq x \leq L_x \quad (s = e, i).$$

A typical set of computed results using the fast and slow scalings is given in Fig. 1. Note that the time scale for the graphs on the left bear no relation to the scale used for the graphs on the right. The first row shows magnetosonic shocks as observed in the simulations [7]. The second row is a validation check on our computations, showing two independent fluid shock tube solutions obtained for neutral gases by setting the electric charge  $e = 0$  as obtained in ref. [7]. The last row depicts magnetosonic solitons. The curves for  $E_x, E_{px}$  and  $\phi$  provide a validation check on our code since the

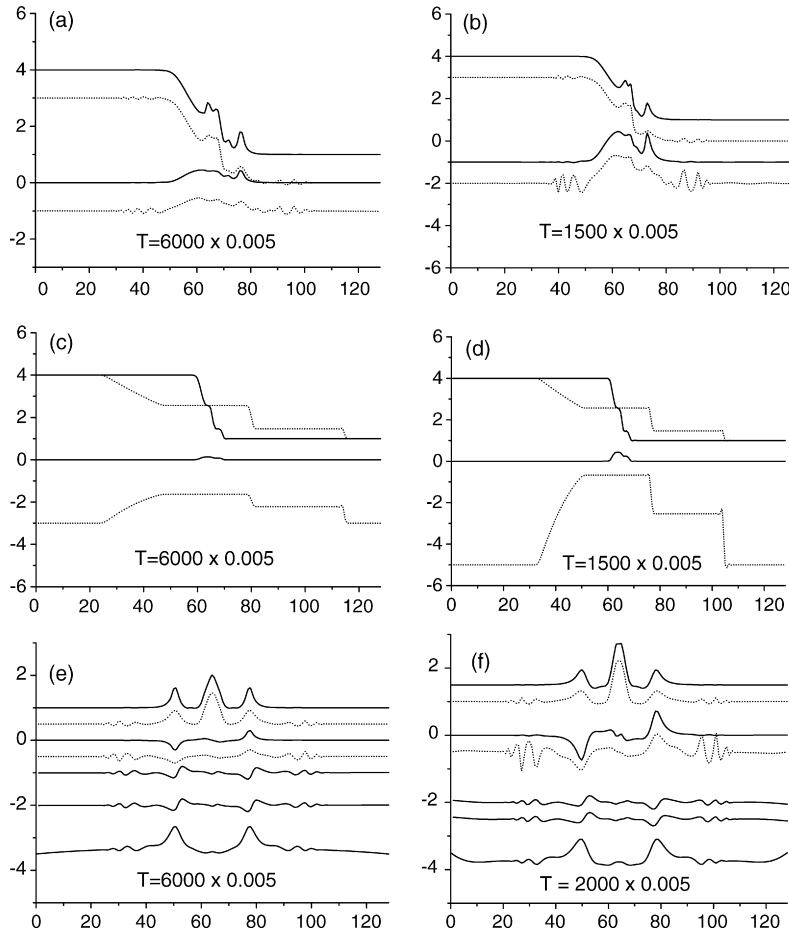


Fig. 1. Shocks and solitons in a two-fluid plasma. The curves on the left arise from  $e$ -scale normalizations and those on the right are  $i$ -scaled. All quantities are in normalized units, as functions of the horizontal  $x$ -values. The curve (a) indicate from top to bottom:  $n_i, n_e - 1, n_i v_{ix}, n_e v_{ex} - 1$ . The curve (b) indicate  $n_i, n_e - 1, n_i v_{ix} - 1, n_e v_{ex} - 2$ . The curves (c) and (d) indicate  $n_i, n_e, n_i v_{ix}, n_e v_{ex} - 5$ . The curve (e) indicate  $n_i, n_e - 0.5, n_i v_{ix}, n_e v_{ex} - 0.5, E_x - 1, E_{px} - 2.0, \phi - 3.5$  with the same except for  $n_i + 0.5, n_e$  in (f).

latter electric field and potential are obtained independently of this scheme by solving a ‘time-frozen’ Poisson equation. Added confirmation that these solutions depict real physical nonlinear waves, is obtained by comparing the nonlinear wave speeds estimated from the graphs above with those from the dispersion relation for linear magnetosonic waves. For the latter we employ [3], the dispersion relation for a magnetosonic wave propagating in a direction perpendicular to an ambient magnetic field  $B_0 (= B_y)$ ,

$$\frac{\omega^2}{k^2} = v_m^2 = c^2 \frac{v_s^2 + v_A^2}{c^2 + v_A^2} \quad (13)$$

where  $v_s$  is the acoustic velocity,  $v_A$  the Alfvén velocity for a wave propagating parallel to the  $B_y$  and  $v_m = \omega/k$  is the magnetosonic phase velocity. Using our two normalizing schemes, we find for the initial parameter values in our computations the values,  $v_m = \pm 0.435$  ( $e$ -scale) and  $v_m = \pm 1.374$  ( $i$ -scale). The estimated respective shock velocities are 0.53 and 1.60, whilst for solitons we have  $\pm 0.47$  and  $\pm 1.40$ . Thus, both the shocks and solitons travel at supersonic speeds, i.e. they relate to the corresponding linear magnetosonic mode. In general, we find that both scalings depict the same physics, but the  $e$ -scaling allows us to use realistic mass ratios (e.g.  $m_i/m_e = 1836$ ) at the expense of larger evolution times, whilst the  $i$ -scaling gives shorter evolution times and require artificially lower mass ratios for numerical stability.

## 5. Conclusion

We have shown how the method [4] for the numerical integration of hyperbolic systems with source terms may be used to solve the 3-D plasma fluid and electromagnetic field equations as a single system for waves in one dimension, in contrast to an earlier work [7]. In modelling magnetosonic shocks, results consistent with earlier simulations are obtained. For solitons, we have been able to obtain clear isolated pulses as opposed to solitary trains [6]. Additionally, we have related such results to linear theory. Also our computations are based on a fast and a slow time scale with the same model equations, and these remain stable and give essentially the same physical results. Finally, we expect to improve on these investigations by extending similar computations into two- and three-space dimensions.

## References

- [1] S. Baboolal, Finite-difference modeling of solitons induced by a density hump in a plasma multi-fluid, *Math. Comput. Simul.* 55 (2001) 309–316.
- [2] J. Balbas, E. Tadmor, C.C. Wu, Non-oscillatory central schemes for one- and two-dimensional equations I, *J. Comput. Phys.* 201 (2004) 261–285.
- [3] F. Chen, *Introduction to Plasma Physics*, Plenum Press, New York, London, 1974.
- [4] R. Naidoo, S. Baboolal, Numerical integration of the plasma fluid equations with a modification of the second-order Nessyahu-Tadmor central scheme and soliton modeling, *Math. Comput. Simul.* 69 (2005) 457–466.
- [5] H. Nessyahu, E. Tadmor, Non-oscillatory central differencing for hyperbolic conservation laws, *J. Comput. Phys.* 87 (1990) 408–463.
- [6] T. Ogino, S. Takeda, Computer Simulation for the Fast Magnetosonic Solitons, *J. Phys. Soc. Jpn.* 38 (1975) 568–575.
- [7] U. Shumlak, J. Loverich, Approximate Riemann solver for the two-fluid plasma model, *J. Comput. Phys.* 187 (2003) 620–638.